

# The top-down mechanism for body mass – abundance scaling

A. G. Rossberg<sup>1,2\*</sup>, R. Ishii<sup>3</sup>, T. Amemiya<sup>1</sup>, K. Itoh<sup>1</sup>

<sup>1</sup> Yokohama National University, Graduate School of Environment and Information Sciences,  
Yokohama 240-8501, Japan

<sup>2</sup> International Institute for Applied Systems Analysis, 2361 Laxenburg, Austria

<sup>3</sup> Frontier Research Center for Global Change, JAMSTEC, Yokohama 236-0001, Japan

\*Corresponding author. Tel.: +81-45-339-4369, FAX: +81-45-339-4353

E-mail addresses: axel@rossberg.net (A.G.R.), r.ishii@jamstec.go.jp (R.I.)

amemiyat@ynu.ac.jp (T.A.), itohkimi@ynu.ac.jp (K.I.)

submitted 27 Jan 2007, accepted 7 June 2007

*Ecology*, in press

**Abstract:** Scaling relationships between mean body masses and abundances of species in multi-trophic communities continue to be a subject of intense research and debate. The top-down mechanism explored in this paper explains the frequently observed inverse linear relationship between body mass and abundance—i.e., constant biomass—in terms of a balancing of resource biomasses by behaviourally and evolutionary adapting foragers, and the evolutionary response of resources to this foraging pressure.

The mechanism is tested using an allometric, multitrophic community model with a complex food-web structure. It is a statistical model describing the evolutionary and population dynamics of tens to hundreds of species in a uniform way. Particularities of the model are the detailed representation of the evolution and interaction of trophic traits to reproduce topological food-web patterns, prey switching behaviour modeled after experimental observations, and the evolutionary adaptation of attack rates. Model structure and design are discussed.

For model states comparable to natural communities, we find that (i) the body mass – abundance scaling does not depend on the allometric scaling exponent of physiological rates in the form expected from the energetic equivalence rule or other bottom-up theories, (ii) the scaling exponent of abundance as a function of body mass is approximately  $-1$ , independent of the allometric exponent for physiological rates assumed, (iii) removal of top-down control destroys this pattern, and energetic equivalence is recovered. We conclude that the top-down mechanism is active in the model, and that it is a viable alternative to bottom-up mechanisms for controlling body mass – abundance relations in natural communities. Several approaches to test the theory in the field are considered.

**Keywords:** body mass, abundance, allometric scaling, community models, food webs.

# 1 Introduction

Empirical data show the abundances  $N$  and the mean body masses  $M$  of species related by power laws of the form  $N \approx N_0(M/M_0)^{-1+\lambda}$ , where one can set  $M_0 = 1$  kg by convention and  $|\lambda|$  is usually small compared to one (e.g., Sheldon et al., 1972; Damuth, 1981; Rodriguez and Mullin, 1986; Nee et al., 1991; Marquet, 2002; Carbone and Gittleman, 2002; Cohen et al., 2003; Quiñones et al., 2003; Marquet et al., 2005; Mulder et al., 2005). The precise value of  $\lambda$  varies and depends on the precise question asked (Sprules and Munawar, 1986; Brown et al., 2004; Li et al., 2004; Marquet et al., 2005). For stable pelagic ecosystems across trophic levels (e.g. Sheldon et al., 1972; Rodriguez and Mullin, 1986; Sprules and Munawar, 1986; Gaedke, 1992; Quiñones et al., 2003; Cohen et al., 2003), and to some degree also for soil food webs (Mulder et al., 2005), the pattern is particularly clear, with  $\lambda \approx 0$ . These observations suggest four questions: (i) What are the mechanisms that lead to the power laws? (ii) What are the values of  $\lambda$  implied by these mechanisms? (iii) What determines the value of  $N_0$ ? (iv) And what determines the observed scatter by a factor 10-100 up and down around the power laws (Cyr, 2000)? The last question seems to be at the core of the problem of understanding species abundance distributions (Whittaker, 1965; Cyr, 2000) and shall here be set aside, leaving questions (i) to (iii).

Many theories for the origin of the power laws build on the “energetic equivalence” (Nee et al., 1991) between species of different size, first observed by (Damuth, 1981) for herbivorous mammals. The conceived mechanism is fundamentally bottom-up: For physiological reasons, mass-specific metabolic rates scale as  $M^{\zeta_r}$ , and rates per individual as  $M \times M^{\zeta_r} = M^{1+\zeta_r}$  with  $\zeta_r \approx -1/4$ . Thus, an assumed fixed rate  $R$  of energy supply can support at most  $N \sim R/M^{1+\zeta_r}$  individuals, yielding  $-1 + \lambda = -1 - \zeta_r$  and  $\lambda = -\zeta_r \approx 1/4$ . Advanced bottom-up theories (e.g., Platt and Denman, 1977, 1978; Cyr, 2000; Brown et al., 2004; Meehan, 2006) take losses by the transfer of energy from one trophic level to the next into account and arrive, by a combination of quantities such as trophic and metabolic efficiencies and predator-prey mass ratios at  $\lambda \approx 0$  or other values. Characteristic the whole class of bottom-up theories is that they predict  $\lambda$  to be of the form  $\lambda = \lambda_0 - \zeta_r$ , with  $\lambda_0$  independent of  $\zeta_r$ . That is, a change in the allometric exponent for the metabolic rate would lead to a change of equal size for  $\lambda$ , but with the opposite sign.

Criticism of bottom-up theories of this form (Griffiths, 1992; Currie, 1993; Marquet et al., 1995; Blackburn and Gaston, 1999) has pointed out that the nature of the uniform source of energy is left unclear, and that the theories do not explained why this source would provide the same amount of energy to each species at a given trophic level. Leaving this point open, it has been argued (e.g., Blackburn and Gaston, 1999), renders the theories somewhat vacuous.

The review by Blackburn and Gaston (1999) discusses five more mechanisms that have been proposed for body mass – abundance scaling. Three of them relate to observational effects, two to ecological mechanisms. But non of these seems to be strong enough to explain the observed scaling over 10 or more orders of magnitude and a large range of taxa. Duarte et al. (1987) considered limitations of space as the mechanism underlying body mass – abundance scaling. However, the space left between individuals, e.g., in the pelagic communities of the open oligotrophic waters of the ocean (Rodriguez and Mullin, 1986; Quiñones et al., 2003), often seems to be too large for this mechanism to become effective.

Yet another conceivable mechanism had been shortly mentioned by Peters (1983), but seems to have received only little attention since: The biomasses of species might be balanced by consumers to be all of similar size. Thus  $B = M \times N \approx \text{const.}$  and  $\lambda = 0$ . This explanation is fundamentally top-down. Intuitively the idea is clear: If there was a species with an outstanding large (eatable) biomass,

many consumers would adapt their behaviour or evolve to feast on it, thus bringing this species back to the normal biomass level or driving it into extinction.

Some indications for this mechanism to be feasible can be found from the model of Benoît and Rochet (2004), which describes size-dependent trophic interactions within a community modeled by a continuous size spectrum. Benoît and Rochet find  $\lambda \approx 0$  nearly constant while varying parameters, including  $\zeta_r$ . However, in a model by Loeuille and Loreau (2006), which differs from that of Benoît and Rochet among others by resolving individual species and allowing body-masses to evolve,  $\lambda$  depends strongly on model parameters. And Damuth (2007) recently interpreted simulations using a simple model of competition for energy on evolutionary time scales as supportive for the bottom-up mechanism. The question is therefore not so much if the top-down mechanism works in principle, but if it will be active under realistic conditions.

In the following Section, we will first introduce a general model of multitrophic community structure appropriate for studying this question. In order to reduce the dependence of model results on questions whether particular model elements affect the relevant mechanism for body-mass abundance scaling, which is *a priori* difficult to answer, and to make the model more realistic while maintaining generality, construction of the model was lead by the principle to include ideally all those elements which are common across a broad range of ecosystems, preferentially those that are empirically well studied. In particular, all elements contained in the three models discussed above by Benoît and Rochet, Loeuille and Loreau, and Damuth are taken into account, except for ontogenetic growth (Benoît and Rochet). Since the model is rather complex, a detailed description of the model and discussions of parametrization and model design have been referred to an Appendix.

After discussing and comparing several aspects of model-community structure with empirical data (Sec. 3), we demonstrate in Sec. 4 that in the model the prediction  $\lambda = \lambda_0 - \zeta_r$  of bottom-up theories does not hold. Rather, we find  $\lambda \approx 0$  independent of  $\zeta_r$ . Next, we confirm the presence of the top-down mechanism by comparing the model with variants where top-down effects have been artificially removed. Section 5 provides a detailed discussion of how the top-down mechanism works. Based on these results, a simple formula can be set up which, up to a factor  $\approx 100$ , predicts the abundance of arbitrary consumer species in a community in terms of physiological properties of individual species.

## 2 Model

### 2.1 Overall model structure

A list of elements included in the model and references motivating their implementation are given in Tab. 1. The main problem targeted by the model is to describe the structure and population dynamics of a multitrophic community at a single location. However, it turns out that, in order to obtain more realistic community structures, it is useful to model, in a simplified form, also the evolutionary history of this community, and the structure of other communities from which species may invade.

Hence, our model describes the population-dynamics and evolution of four communities, which are weakly coupled by the occasional exchange of species, but population-dynamically uncoupled. It is a statistical model describing tens to hundreds of species in a uniform way. Only “producers” (e.g., algae or plants) and “consumers” (all higher trophic levels) are explicitly distinguished. Since, for reducers in the soil, energy (detritus) is provided largely independent of consumption, just as light for primary producers, reducers in soil ecosystems can take the role of “producers” in the model as well. Each community is characterized by the biomasses  $B_i$  and the mean body masses  $M_i$  of its member species  $i$ , implying population numbers  $N_i = B_i/M_i$ , and by the trophic interaction structure.

Model Element	Based on
Energy conservation and dissipation	McNiel and Lawton, 1970; Peters, 1983
Allometric scaling of physiological rates	McNiel and Lawton, 1970; Peters, 1983; Savage et al., 2004
Type II functional responses	Jeschke et al., 2004
Prey switching	Greenwood and Elton, 1979
Size ratios determining trophic links	Claessen et al., 2002; Brose et al., 2006
Abstract traits determining trophic links	Yoshida, 2003; Rossberg et al., 2006a
Evolution of body masses	Loeuille and Loreau, 2005
Evolution of abstract traits	Yoshida, 2003; Rossberg et al., 2006a
Differentiation of evolution rates by traits	Rossberg et al., 2006a; Bersier and Kehrli, 2007
Community evolution through simplified speciations	Caldarelli et al., 1998, Sec. 2.2
Population-dynamically isolated, evolutionary coupled patches	arguments discussed in Sec. 2.2
Free evolution of attack rates	arguments discussed in Sec. 2.3

Table 1: Elements contained in the population-dynamical matching model

## 2.2 Evolution

On time scales larger than typical population-dynamical times, the species pool of each community evolves—technically by “speciations”, local extinctions, and “invasions” from the three other communities. However, the picture behind these processes, sketched in Fig. 1, is more complex: Each of the four explicitly modeled communities (black “lakes” in Fig. 1) has a number of similar communities in its vicinity that are not explicitly modeled (gray “lakes”). Most speciations are allopatric and occur within these surrounding communities, at times and for reasons unrelated to the explicitly modeled communities. But species invading a modeled community from its surrounding will often have some similarity with species already present due to common evolutionary ancestors. Thus, from the perspective of the local community, such invasions will appear as if they were spontaneous “speciations” of existing species by large mutations. Furthermore, “invasions” from the other three modeled communities (arrows in Fig. 1) proceed in steps through other systems, thus giving rise to some evolutionary variation and some delay, and decoupling the population dynamics of the four modeled communities. Thus, “speciations” and “invasions” in the model are extremely coarse-grained descriptions of the actual evolutionary processes. It can be shown that this coarse graining of phylogeny in models of local communities affects food-web topology only weakly (Rossberg, 2007). Except for some sympatric speciations, both local “speciations” and “invasions” correspond, in reality, to invasions of the community by species more or less related to existing ones. We shall denote these processes below collectively as *additions* to a community, and use the number of *species added* (abbreviated as ‘s.a.’) as a measure of evolutionary time.

## 2.3 Attack rates

Traits mutating in speciations include not only body masses and abstract foraging and vulnerability traits, which together determine feeding relationships, but also the attack rates of consumers. Attack rates can evolve freely in the model without an explicit physiological tradeoff. As is shown below,

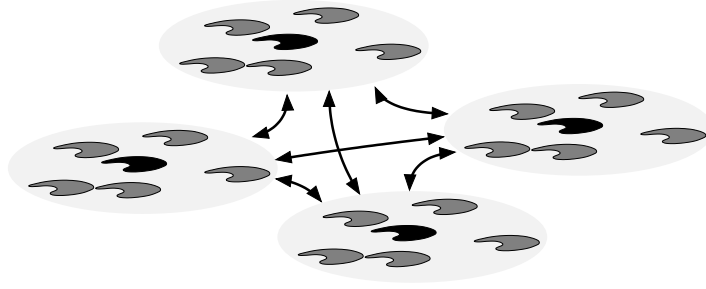


Figure 1: The hierarchical spatial structure assumed in the evolutionary sub-model. See Sec. 2.2 for explanations.

mean attack rates of communities will nevertheless evolve to some stable value, well below the point of total eradication of all producers, but sufficiently large to control resource populations. This is not to imply that attack rates in nature cannot also be determined by physiological and physical constraints, but this mechanism is here excluded for simplicity.

## 2.4 Parametrization

Empirical estimates for model parameters were used whenever possible, and model variables are expressed in physical units. This allows a quantitative comparison of macroecological model properties (e.g., biomass densities) with empirical data. If there was a choice, we preferred parameter values applicable to pelagic communities, because (i) for pelagic communities the empirical pattern of body mass – abundance scaling is particularly clear, (ii) due to their relatively high spacial homogeneity they might be comparatively easy to model, (iii) in the present form the model favors primary producers of small body mass resembling phytoplankton (see, however, Sec. 4.3.3). Interpretations of model states in terms of pelagic communities therefore come easily to mind, and we shall sometimes invoke them below. Yet, in order to maintain generality, the model was intentionally constructed such as not to include elements specific to and should not be misunderstood as an attempt to quantitatively reproduce the properties of particular community types.

Masses are expressed in the currency of wet biomass—and biologically available energy is assumed proportional to mass—since this is the traditional choice of allometric theory (Peters, 1983). This choice obviously raises some conceptual and quantitative issues, but at the degree of accuracy targeted here, these are not relevant, yet.

The Appendix first gives a complete definition of the model. It then provides a detailed discussion of specific model design decisions, the rational behind choices of parameter values, and a full list of model parameters and variables.

## 3 General Properties of Model Communities and their Dynamics

The purpose of the sections is twofold. It provides information on general model community structure that is referred to in the discussion of body mass – abundance scaling further below, and, by comparison with empirical results, it offers a picture of the degree of realism that is reached by the model and points out possible artifacts.

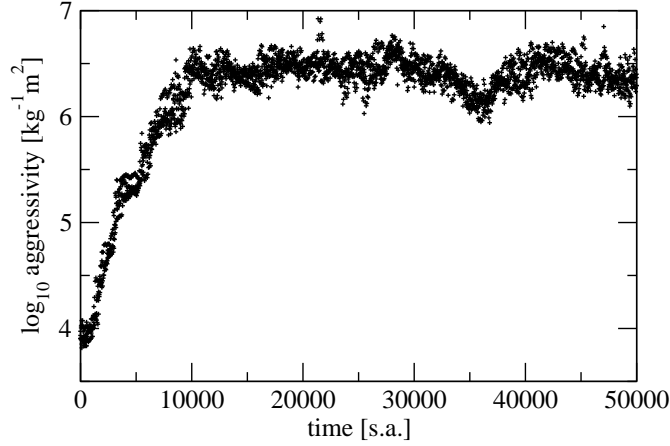


Figure 2: Time series of the mean consumer aggressivity  $g$ , the attack rate normalized to consumer respiration rate and system area. Samples (+) are taken in each community after every 60 s.a. (species added).

### 3.1 Evolution of attack rates and steady state

Simulations of the model show that at the community level attack rates evolve to a stable evolutionary equilibrium. We define the aggressivity  $g_i$  of a species  $i$  as  $g_i = a_i A / r_i$ , i.e., as the attack rate  $a_i$  normalized to the system area  $A$  and the specific respiration rate  $r_i$ . The aggressivity has dimensions of an inverse biomass density. Figure 2 shows a time series of the community means of the aggressivity  $g$  for standard parameters as listed in the Appendix. After a transient with exponential growth, the aggressivity settles in at  $(3 \pm 2) \times 10^6 \text{ kg}^{-1} \text{ m}^2$ , where we employ a notation ‘mean  $\pm$  standard deviation’.

After the aggressivity saturates, other system properties, such as the number of species, reach their steady-state values as well. Characterizations of the steady state below are based on the data from 18,000 s.a. to 80,000 s.a., where the simulations were stopped.

### 3.2 Fluctuations in the evolutionary steady state

In the steady state, each community consists of  $S_p = 46 \pm 14$  producer species and  $S_c = 24 \pm 8$  consumer species on the average. Figure 3 displays the time series of  $S_p$  and  $S_c$  for one of the four communities. Immediately apparent are the strong fluctuations, which are due to intermittent extinction avalanches, not unlike those found in the paleontological record (e.g. Solé et al., 1997). Amaral and Meyer (1999) observed such extinction avalanches also in a simplified model for the evolution of food-web topology. Many later models combining evolutionary and population dynamics did not produce large extinction avalanches (Drossel et al., 2001; Yoshida, 2003; Loeuille and Loreau, 2005, 2006). It is not clear if the avalanches found in the model correspond to those observed.

Other quantities, such as the aggressivity displayed in Fig. 2, also exhibit fluctuation over long time scales (thousands of s.a.). The resulting temporal correlations affect the accuracy of characterizations of the steady state, which is, e.g., reflected in the residual scatter of the simulation results for  $\lambda$  in Fig. 8 below.

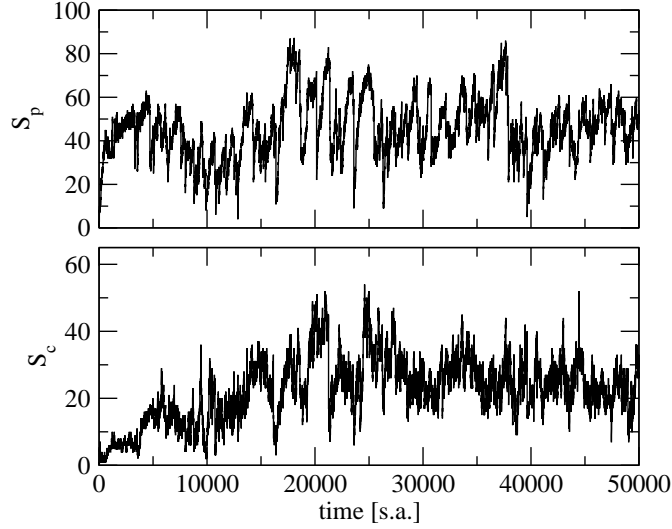


Figure 3: Time series of the number of producer species  $S_p$  and the number of consumer species  $S_c$  in one of the four communities.

### 3.3 Distribution of body masses

The average number of species in each logarithmic body size class is shown in Fig. 4. In the presence of herbivory, producer body masses tend to evolve towards the lowest allowed value in the model  $M_{\min} = 10^{-13}$  kg (but see Sec. 4.3.3 for the case without herbivory). Thus, almost all producers fall into the smallest size class. The average maximum body mass in a community is  $10^{-0.5 \pm 2.0}$  kg. This upper limit for the body mass is partially due to the finite habitat size, and partially due to energetic or dynamic constraints along the food chain. The hard-coded upper limit of the model  $M_{\max} = 10^3$  kg only marginally affects this value.

In empirical data for lakes (e.g., Jonsson et al., 2005), the body masses of producer species easily span two orders of magnitude. The extremely sharp distribution found here is certainly a consequence of the sharp lower body-mass cutoff employed in the model. On the other hand, the maximum of the consumer species distribution near  $10^{-9}$  kg has been found empirically in similar form by Jonsson et al. (2005), and the secondary peak near  $10^{-2}$  kg, corresponding to fish species, as well, albeit sharper than here.

### 3.4 Typical population dynamics in the steady state

After the perturbations arising when species are added to the communities have relaxed, populations typically exhibit chaotic, and occasionally also periodic, oscillations. Due to their small body masses and the resulting fast population dynamics, the variability of the biomasses of producers is much larger than that for most consumers. Figure 5 displays a typical time series for the producer biomasses in a community. Some producers appear to follow “K-strategies” (small variability) others “r-strategies” (algae blooms), with biomasses spanning four orders of magnitude or more (typical values of  $\text{std log}_{10} B_i$  are in the range  $0.5 \dots 1.5$ ). The duration of the blooming events is on the order of weeks, compatible with observations in pelagic communities. The intensity of blooming shows no seasonal variability because seasonal effects are not modeled. Due to their larger body masses, the

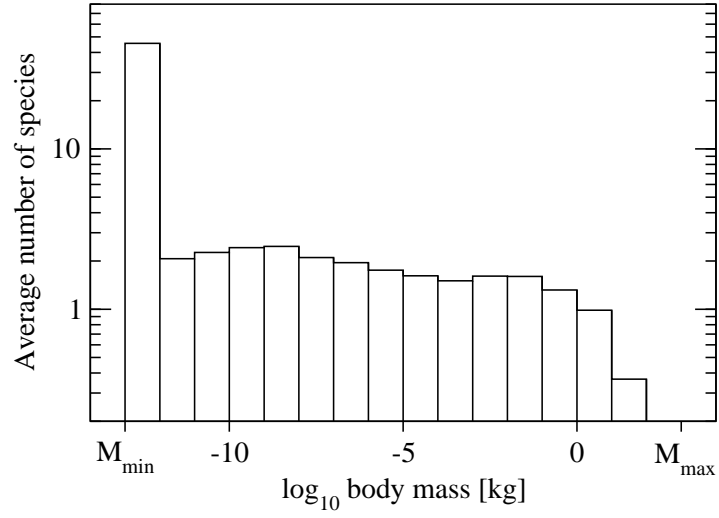


Figure 4: Average number of species in each decimal size class in the model steady state.

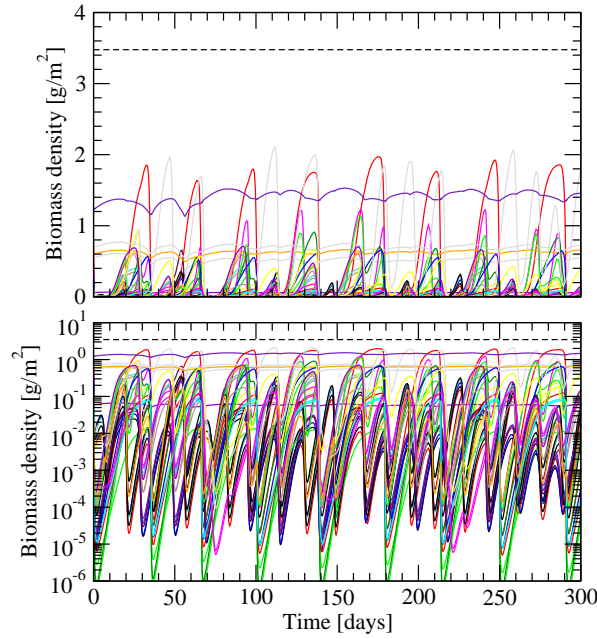


Figure 5: Typical chaotic variations of producer (e.g., phytoplankton) biomasses in the model steady state, parameters as given in the Appendix. Lines of different color or gray level correspond to different species. The same data is shown on a linear scale (top) and a logarithmic scale (bottom) for comparison. The dashed horizontal line corresponds to the monoculture carrying capacity for the smallest producer species.

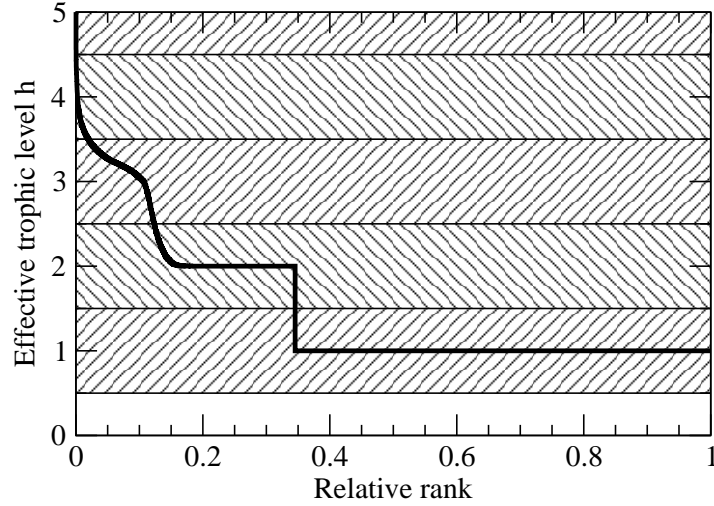


Figure 6: The effective trophic level  $h$  of species vs. their relative rank in the steady state of the model. Producers correspond to  $h = 1$ . Shadings indicate the corresponding integer trophic levels obtained by rounding  $h$ .

variability of consumer biomasses is much smaller (typically  $\text{std } \log_{10} B_i < 0.3$ ).

Results below always refer to time averages of biomasses  $B_i$  and trophic mass flows ( $f_{ij}B_j$  in the formalism of the Appendix), obtained numerically from simulations of population dynamics.

### 3.5 Distribution of trophic levels

Figure 6 shows the effective trophic level  $h$  (Levine, 1980) vs. its relative rank. Specifically, the effective trophic levels of all species from all communities, sampled every 60 s.a. in the steady state, are ordered from large to small, and the ranks in this order are normalized by dividing by the total number of sampled species. The cumulative probability distribution can be obtained from this graph by a simple exchange of axis. This representation of the level structure was chosen for an easy comparison with the corresponding empirical result of Christian and Luczkovich (1999) for a seagrass community, who found that “The effective trophic levels of consumers tended to aggregate near integer values, but the spread from integer values increased with increasing level.” The same phenomenon is found in simulations. This partially quantized structure justifies the grouping of species into trophic levels (producers, herbivores, carnivores, super-carnivores) according to the integer value nearest to  $h$ . The average community maximum effective trophic level is  $h_{\max} = 3.7 \pm 0.4$  in the steady state. Effective trophic levels larger than 4.5 are rarely observed.

### 3.6 Topological properties of model food webs

Food-web topologies were obtained by considering exactly those resources as linked to a consumer that contribute more than 1% to the consumer’s diet (Drossel et al., 2004). A theoretically important property of food webs (May, 1972) is the number of links per species, the link density  $Z$ . We obtain  $Z = 4.1 \pm 1.3$ . For a better comparison with empirical data on food web topology,  $Z$  and the topological food-web properties listed in Tab. 2 have been computed after the following standardization

Symbol	Simple Explanation	Model	Observations
$S$	number of species	$20 \pm 8$	$54 \pm 35$
$C$	directed connectance	$0.21 \pm 0.05$	$0.16 \pm 0.10$
$T$	fraction of top species	$0.15 \pm 0.09$	$0.18 \pm 0.19$
$GenSD$	variability of generality	$0.91 \pm 0.12$	$1.13 \pm 0.44$
$VulSD$	variability of vulnerability	$0.84 \pm 0.16$	$0.98 \pm 0.18$
$MxSim$	trophic similarity among species	$0.62 \pm 0.07$	$0.60 \pm 0.10$
$Cannib$	fraction of cannibal species	$0.37 \pm 0.09$	$0.16 \pm 0.19$
$aChnLg$	mean food-chain length	$3.9 \pm 1.4$	$6.4 \pm 4.1$
$aChnSD$	variability of chain length	$1.3 \pm 0.3$	$1.6 \pm 0.7$
$aChnNo$	$\log_{10}$ number of chains	$2.6 \pm 0.8$	$4.3 \pm 2.2$
$aLoop$	number of loops	$3 \pm 3$	$11 \pm 20$
$aOmniv$	degree of omnivory	$0.74 \pm 0.13$	$1.0 \pm 0.33$
$Ddiet$	deviation from intervality	$0.33 \pm 0.20$	$0.22 \pm 0.15$
$Clust$	clustering coefficient	$0.53 \pm 0.11$	$0.50 \pm 0.15$

Table 2: Topological properties of model food webs in the steady state ( $\pm$  standard deviations) at standard parameters (see Appendix), compared to the ranges of values found in an analysis of 17 empirical data sets. For sources of empirical data, precise definitions of the properties, computational issues, and individual values, see Rossberg et al. (2006a).

of the raw topological data: First, small unconnected sub-webs are removed (Williams and Martinez, 2000), then, all producers are lumped into a single species, and finally species with the same sets of consumers and resources are lumped together as “trophic species” (Cohen et al., 1990) (for motivation and discussion, see Rossberg et al., 2006a).

A quantity related to  $Z$  is the average number of resources of a consumer, the consumer link density  $Z_c$  ( $= 8 \pm 2$  in the steady state). Since this quantity is directly empirically accessible without sampling a complete web (Rossberg et al., 2006b), no standardization of food-web topology was done to compute it.

Large link densities, as we find them here in good accordance with empirical data (Dunne et al., 2002; Banašek-Richter et al., 2005; Rossberg et al., 2006b), are known to be difficult to reproduce in complex population-dynamical models. For example, link densities in the models investigated by Drossel et al. (2004) do not exceed<sup>1</sup> 2.3. The present model would not yield large link densities either, if the known stabilizing effect of prey switching (Oaten and Murdoch, 1975) had not been included. Large link densities, on the other hand, might be important for the top-down mechanism, since they allow consumers to compare and to balance biomasses between resource species.

Means and standard deviations of other topological properties of model food webs in the steady state are listed in Tab. 2 for reference. For a simple comparison with empirical data, means and standard deviations of the corresponding values obtained from a collection of 17 empirical data sets are listed as well. Of the 14 properties, the model averages of 13 are within one standard deviation of the empirical range. Model webs have a comparatively large fraction of cannibal species (*Cannib*), but cannibalism is known often to be underreported (Cohen et al., 1990). All 14 model averages are within two standard deviations of the empirical data. This shows that the topology of the model food webs does not exhibit any obvious artifacts that might favor the top-down mechanism. A more

<sup>1</sup>In other work, larger values are reported, but these generally include all links regardless of their strength.

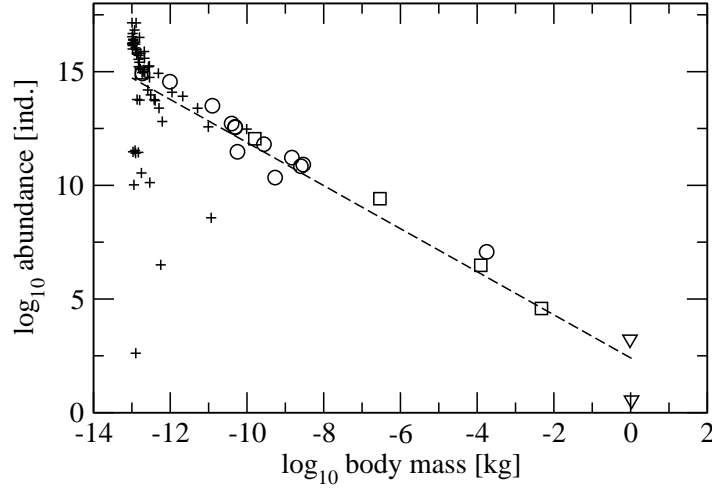


Figure 7: Typical body mass – abundance relation in a model community, parameters as given in the Appendix. Points denote population sizes of individual species. The dashed line corresponds to a linear regression ( $N \sim M^{-0.95}$ ). Symbols encode trophic levels:  $+$ =1 (producers),  $\circ$ =2 (herbivores),  $\square$ =3 (carnivores),  $\nabla$ =4 (super carnivores).

systematic validation of the model food-web topology is desirable but beyond the purpose of the current work.

## 4 Numerical Experiments and Results

### 4.1 Definition of scaling exponents

There are two different approaches commonly used for defining the scaling exponent. One is a double-logarithmic regression of the normalized size spectrum (Platt and Denman, 1977, 1978), where the size spectrum is obtained by first determining the total biomasses of all individuals in logarithmically scaled size classes and then dividing these totals by the width of the classes (which yields values of dimension abundance). The other approach is a direct double-logarithmic regression of the abundances or biomasses of all species with their mean body masses (Damuth, 1981), usually taking body mass as the independent variable. The first approach is much easier to realize in field studies, in particular if the number of species is large. However, in small communities the size spectrum may have gaps with unoccupied size classes (Havlicek and Carpenter, 2001), leading to singularities when taking logarithms. The second approach does not have this conceptual disadvantage, and is more robust when the number of species is small. The precise relationship between the two definitions is not clear. Below, results for both definitions are given. All regressions reported are ordinary least square with  $\log_{10} M$  as the independent variable.

## 4.2 Body mass vs abundance scaling in simulated food webs

### 4.2.1 Direct regression

For a typical model community, the body masses and time-averaged abundances of all species, as well as their trophic levels, are shown in Fig. 7. Direct double-logarithmic regression yields a relation  $N \sim M^{-1+\lambda}$ , or  $B = N \times M = M^\lambda$ , with  $\lambda = 0.05$  ( $n = 79$ , nominal standard error: 0.09).

When pooling the data of all saved steady-state communities of the model run with standard parameters (see Appendix), the corresponding value is  $\lambda = -0.002$  ( $n = 279598$ ). When restricting the regression to consumer species, the exponent in the relation  $B \sim M^{\lambda_c}$  is  $\lambda_c = 0.034$  ( $n = 96276$ ). Because of strong phylogenetic and temporal correlations, which are difficult to take into account, we refrain here from computing error estimates from the underlying data. From the comparison of different simulation runs below, the standard error in  $\lambda$  and  $\lambda_c$  can be estimated as  $\approx 0.02$ .

As has explained in Sec. 1, bottom-up theories, such as the energetic equivalence rule, predict that the scaling exponent  $\lambda$  in the relation  $B = M \times N \sim M^\lambda$  is of the form  $\lambda = \lambda_0 - \zeta_r$ , where  $\zeta_r$  is the allometric exponent for the mass-specific metabolic rates of consumers. The current model incorporates the metabolic rates of consumer species in their respiration rates and their maximum growth rates (see Appendix).

To test if bottom-up theories apply to the current model, we considered a modification of the model where the allometric exponent of consumer metabolic rates  $\zeta_r$  is replaced by alternative values  $\zeta_r = -0.35 \dots -0.15$ . The coefficients of the corresponding scaling laws were adjusted in such a way as to keep rates constant at  $M_i = 10^{-10}$  kg, near the lower end of the range occupied by consumers in the model.

This modification is a compromise between leaving as many parts of the model unchanged for better comparison with the main simulation, and consistently implementing a thought experiment to test bottom-up theories. As a result, the allometric exponents for producer physiological rates and for the background scaling of attack rates (Eq. A11 in Appendix), on one hand, and for consumer physiology, on the other hand, differ. But the former exponents only weakly affect the community structure: The value of the allometric exponent for producer physiological rates has little effect, since most producers have body masses near  $M_{\min}$ , and the effective exponent for the attack rates can be adjusted by the evolutionary mechanism.

The range of values over which  $\zeta_r$  can reasonably be varied is limited. At the upper end ( $\zeta_r = -0.15$ ) of the range investigated, the number of consumer species  $S_c = 16 \pm 9$  is low, and lowering it further will destroy system-level effects resulting from the interaction of many species. At the lower end ( $\zeta_r = -0.35$ ) the range of consumer body masses spreads out widely and is limited from above by the condition  $B_i > M_i$ . Reducing  $\zeta_r$  further would potentially bias the  $B_i$ . Furthermore, species numbers become large ( $S_c + S_p = 144$  on average) and simulations difficult. In fact, the computations for  $\zeta_r = -0.35$  had to be stopped prematurely after 29000 s.a. or 716 hours of simulations. But we expect that the large number of consumer species  $S_c = 75 \pm 31$  in the communities for  $\zeta_r = -0.35$  mostly compensates a possible losses of accuracy in  $\lambda$  and  $\lambda_c$  due to the reduced simulation time.

The simulation results displayed in Fig. 8 show no obvious relationship between  $\lambda$  and  $\zeta_r$  or between  $\lambda_c$  and  $\zeta_r$ . A statistical analysis confirms this impression: Linear regression yields  $\lambda = -0.032(27) - 0.06(10)\zeta_r$  ( $n = 7$ , standard errors in parenthesis, residual std 0.016) and  $\lambda_c = 0.036(36) + 0.14(14)\zeta_r$  (residual std 0.021).<sup>2</sup> The null hypothesis that  $\lambda = \lambda_0 - \zeta_r$  with fixed  $\lambda_0$  is rejected ( $p = 0.0003$ ), the corresponding hypothesis for  $\lambda_c$  as well ( $p = 0.0004$ ). Instead, the

<sup>2</sup>Estimates and standard errors have similar values by chance.

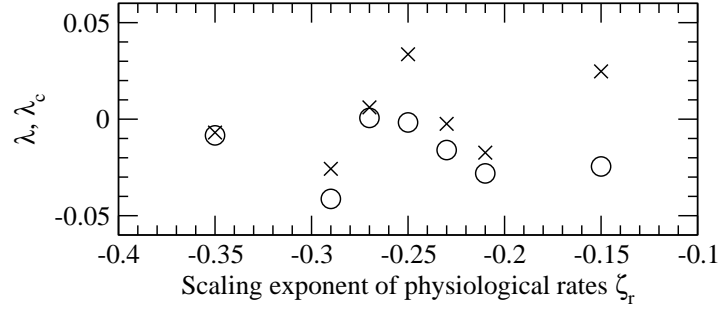


Figure 8: Simulation results for the scaling exponent relating biomass as  $B \sim M^\lambda$  to body mass  $M$  for varying allometric exponent  $\zeta_r$  of consumer physiological rates. (○:  $\lambda$  all species, ×:  $\lambda_c$ , consumers only). Horizontal and vertical axis are drawn at the same scale.

data is compatible with the null hypothesis' that  $\lambda$  and  $\lambda_c$  are independent of  $\zeta_r$  ( $p = 0.3$  and  $p = 0.4$ , respectively) with means  $-0.017(6)$  for  $\lambda$  and  $0.002(8)$  for  $\lambda_c$ . The latter value is consistent with zero (two-sided t-test,  $p = 0.8$ ), while the former is rather not ( $p = 0.025$ ).

#### 4.2.2 Regression of size spectra

For reasons discussed in Sec. 4.1, scaling exponents based on size spectra become ill defined if the number of species is small. Besides, producer biomasses exhibit a larger variability than consumer biomasses (see Fig. 12 below), leading to non-power law size spectra if producers are included. The analysis here is therefore restricted to consumer species, and for each value of  $\zeta_r$  the mean slope  $\bar{\nu}_c$  is computed as the arithmetic mean of the slopes of the normalized size spectra of only the  $n = 100$  steady-state communities with largest number of consumers  $S_c$ . Choosing  $n = 50$  or  $n = 200$  instead does not alter the statistical conclusions. Species were grouped in decimal size classes to compute the spectra. Figure 9 displays the slopes  $\nu_c$  of normalized steady-state size spectra ( $\zeta_r = -0.25$ ) vs.  $S_c$  and the  $n = 100$  cutoff.

Mean slopes  $\bar{\nu}_c$  for varying  $\zeta_r$  are shown in Fig. 10. Again, there is no clear relationship. Linear regression gives  $\bar{\nu}_c = -1.061(30) - 0.04(11) \zeta_r$ . Here, too, the null hypothesis that  $\bar{\nu}_c = \nu_0 - \zeta_r$  with fixed  $\nu_0$  is rejected ( $p = 0.0004$ ) and the hypothesis of constant  $\bar{\nu}_c$  is accepted ( $p = 0.7$ ). The mean value of  $\bar{\nu}_c$  over all  $\zeta_r$  is  $-1.050(7)$ , slightly but significantly smaller than  $-1$  ( $p = 2 \cdot 10^{-4}$ ).

If consumer abundances would scale exactly as  $N \sim M^{-1+\lambda_c}$  and consumer species were distributed evenly over the  $M$  axis, a relation  $\nu_c = -1 + \lambda_c$  would hold. The fact that simulated spectra have slightly steeper slopes is consistent with expectation, since there are more small than large species. Slopes of empirical size spectra tend to be slightly smaller than one as well (Quñones et al., 2003).

### 4.3 Testing the top-down theory for body mass – abundance scaling

#### 4.3.1 The distribution of species in the body mass – biomass plane

In order to understand the weak dependence of  $\lambda$  on  $\zeta_r$ , it is instructive to inspect the underlying distribution of species in the  $\log B$ ,  $\log M$  plane. Steady-state densities in the  $\log M$ - $\log B$  plane

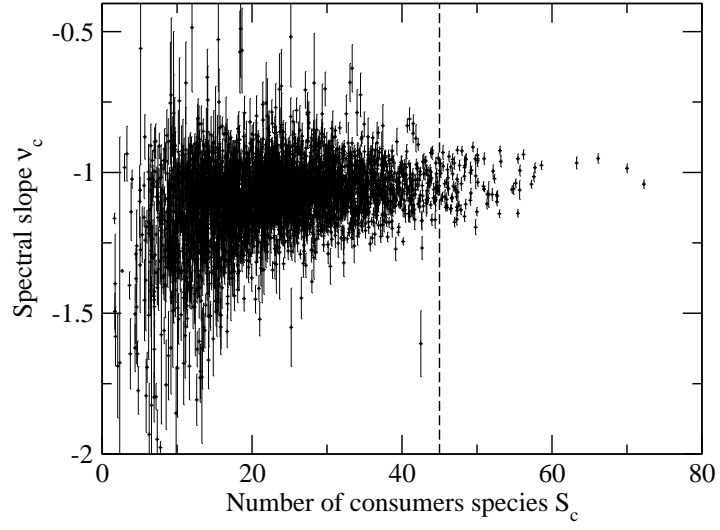


Figure 9: Slopes of model consumer size spectra vs. consumer species richness  $S_c$ . Parameters as in Appendix. Error bars indicate sample estimates of standard errors. The 100 communities to the right of the dashed line have an average slope of  $-1.04$ .

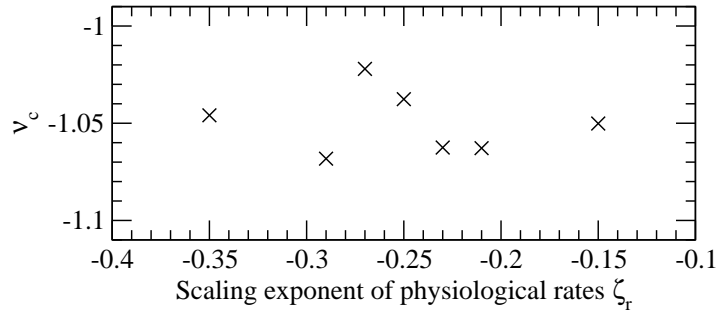


Figure 10: Simulation results for slopes of consumer size spectra vs. the allometric exponent  $\zeta_r$  of consumer physiological rates. Horizontal and vertical axis are drawn at the same scale.

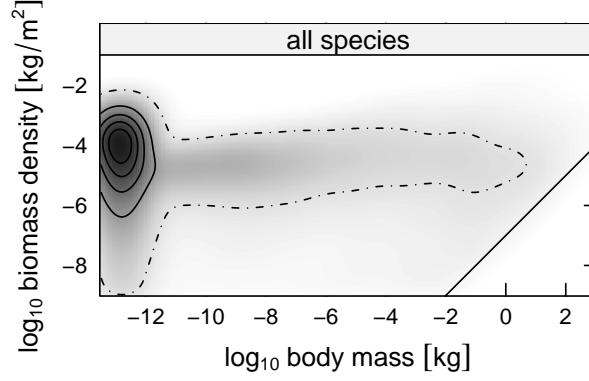


Figure 11: Estimated density of species in the body mass – biomass plane for the model steady state, parameters as given in the Appendix. The four solid level lines correspond to 80%, 60%, 40%, and 20% of the maximum density. The dash-dotted line corresponds to 2.5%. Gray levels encode intermediate densities. The solid line in the lower right corner corresponds to the extinction limit at  $B = M$ . The peak of the distribution at low body masses, which is dominated by producer species, is blurred by the smoothing window. With a narrower window, the long tail towards higher body masses would become invisible. For the actual density of producer species, see the top panel of Fig. 12.

(Figs. 12-14) were estimated using a kernel estimator applied with equal weight to all species contained in snapshots taken over the evolutionary model steady states of all four communities every 60 s.a.. In order to avoid biases from the kernel, it was chosen data driven as a bivariate normal density with covariance matrix  $1.5 \mathbf{C} N^{-1/3}$ , where  $\mathbf{C}$  is the estimated covariance matrix of the data and  $N$  the number of sample points. The exponent  $-1/3$  guarantees a balance between stochastic errors and errors due to smoothing for bivariate distributions.

The distribution of species in the  $\log B$ ,  $\log M$  plane is shown in Fig. 11 (standard parameters). Apparent are the region of high density at low body masses corresponding to producer species, and the long tail with roughly constant biomass stretching towards higher body masses. A more detailed picture can be obtained by splitting this distribution into the contributions from different trophic levels. This has been done in Fig. 12. The maxima of the distributions for all levels are located near a line of constant  $B$ . The positions of the maxima are listed in Tab. 3. The regression line through these points yields a between-level slope of  $-0.037$ . For herbivores and carnivores, the within-level slopes are also close to zero (Tab. 3). For super carnivores, the slope (0.144) is closer to 0.25 than to 0. However, Fig. 12 suggests that this is rather due to the extinction limit at  $B = M$  (i.e.,  $N = 1$ ) than due to the structure of the bulk of the distribution.

	maximum at		slope of regression $\log B$ on $\log M$
	$\log M$ [kg]	$\log B/A$ [ $\text{kg m}^{-2}$ ]	
producers	-12.8	-4.0	(-2.1)
herbivores	-10.3	-4.6	0.017
carnivores	-8.6	-4.8	0.050
super carnivores	-1.4	-4.6	0.144

Table 3: Characteristics of distributions displayed in Fig. 12.

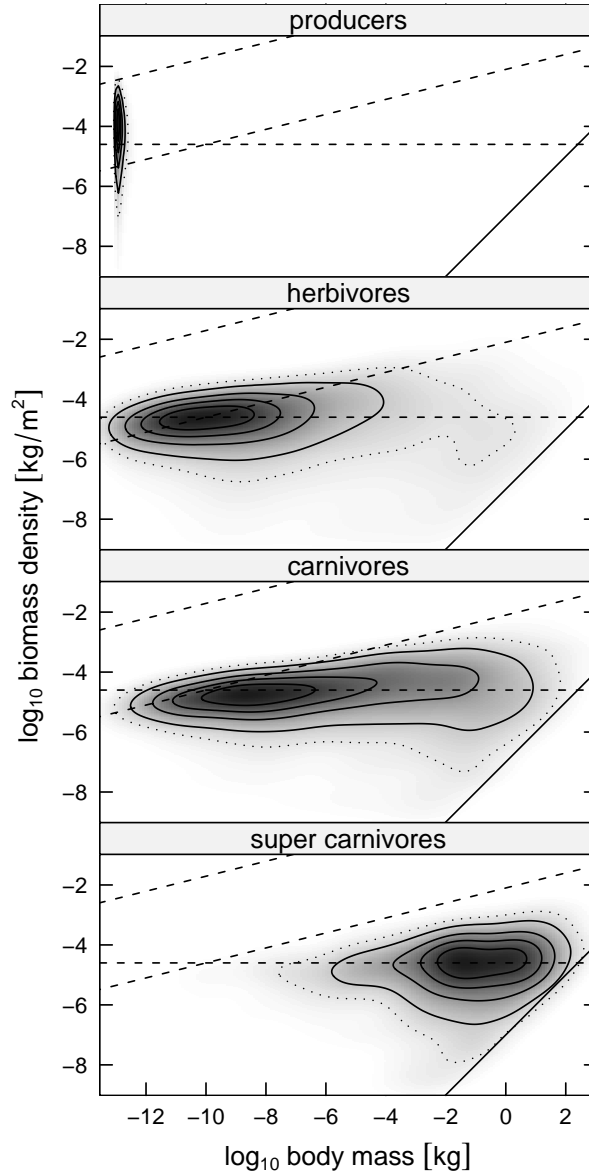


Figure 12: Density of species in the body mass – biomass plane, separated by trophic level, in the steady state of the model, parameters as given in the Appendix. The four solid level lines correspond to 80%, 60%, 40%, and 20% of the maximum density. The dotted line corresponds to 10%. Gray levels encode intermediate densities. The solid line in the lower right corner corresponds to the extinction limit at  $B = M$ . The dashed line in the upper left corner represents the carrying capacity for producer species in monoculture. The two other dashed lines are guides to the eye with slopes 0 and 1/4, respectively. All auxiliary lines are reproduced identically in Figs. 13 and 14. Horizontal and vertical axis are drawn at the same scale.

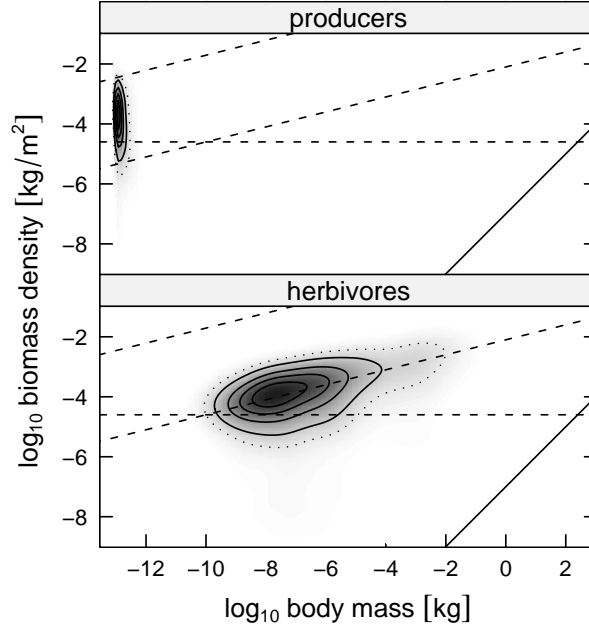


Figure 13: Density of species in the body mass – biomass plane, separated by trophic level. Model variant without carnivores. See Fig. 12 for details.

#### 4.3.2 Communities without carnivores

To test the hypothesis that the distribution of species in the  $\log B$ ,  $\log M$  plane is under top-down control, top-down effects were disabled in the model in two steps. First, carnivory was disabled. That is, in a modification of the original model, the trophic interaction coefficients  $c_{ki}$  were set to zero whenever the resource species  $k$  was a consumer. The remaining trophic interactions were only between consumers (herbivores) and producers. Figure 13 shows the distributions of producers and consumers in the  $\log B$ - $\log M$  plane for this case. The bulk of the distribution for consumers now stretches along an energetic equivalence line (slope 1/4), rather than a line of constant biomass as was the case in the full model. The numerical value obtained for the slope by ordinary least square regression is somewhat smaller (0.153), which can be attributed to the comparatively large scatter along  $\log B$ , but it is still closer to 1/4 than to zero.

#### 4.3.3 Communities without consumers

Similar observations can be made when disabling also herbivory, and running the model only with producer species. Released from the need to compensate losses by grazing at the highest possible rate, larger producers can now evolve. In fact, inter-producer competition is modeled such that larger producers have a competitive advantage over smaller producers (Eqs. (A5),(A6) in Appendix): A large producer at its carrying capacity depletes a large part of the resources of a small producer if there is sufficient niche overlap, while a small producer at its carrying capacity has only a weak effect on the resources available to a large producer. As a result, producers evolve to larger sizes, limited, in this model, only by the system size or the hard upper cutoff  $M_{\max}$ . Producer biomasses are close to their monoculture carrying capacities (Fig. 14, upper dashed line), in good agreement with the energetic

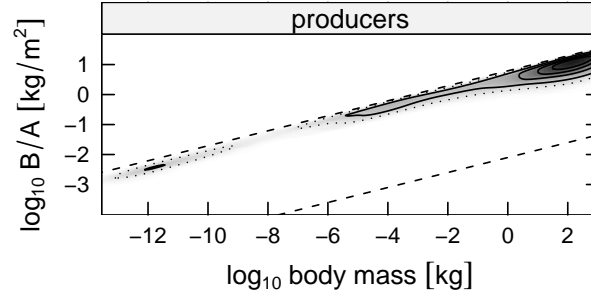


Figure 14: Density of producers in the body mass – biomass plane. Model variant without consumers. See Fig. 12 for details.

equivalence rule.

That is, in the absence of consumption, the structure of the producer community resembles rather a forest than a planktonic community. As an aside, a similar observation can be made if, in the model, producers are allowed to evolve vulnerability traits that cannot easily be matched by the foraging traits of consumers. In the presence of consumption, trees can evolve only if equipped with a sufficiently effective defense, just as observed in nature.

The small scatter away from the energetic equivalence line in Fig. 14 might at first be surprising. It can be attributed to the simplicity of the producer sub-model: Apart from the scaling of rates and carrying capacities with body size, the population dynamics of different plant species are identical when niche overlaps are sufficiently small. The situation without carnivores (Fig. 13) is not quite as simple. Consumers differ in their attack (or grazing) rates, the degree of adaptation to, and the abundance of their resources. It is remarkable that energetic equivalence is approximately realized in these communities, too.

## 5 Discussion

The results discussed above show that in the model (i) the body mass – abundance scaling exponent does not change with the allometric scaling of the metabolic rates in the form predicted by bottom-up theories, (ii) rather, the dependence of the exponent on the allometric scaling of the metabolic rate is weak, (iii) the scaling exponent of abundance with body mass is close to  $-1$  over a wide parameter range, which implies that the biomass of species does not depend systematically on their body mass, and (iv) this scaling breaks down if top-down control is disabled. These results show that in the model the top-down mechanism is active: the biomasses of species are in an equilibrium mediated by adaptive foraging.

Top-down control can explain why biomasses are limited from above by some equilibrium value. Together with a general heuristic argument, it can also explain why biomasses are, on a logarithmic scale, located *near* this equilibrium value: In order for the population of a species to saturate at some value, a mechanism for density dependent population growth is necessary. In the model, such density dependent mechanisms set in when a species either controls the abundance of its main resources, such that an increase of its own abundance will lead to a depletion of the resource, or when this species is the main resource for some consumer, and thus determines the abundance of the consumer and its own

consumption rate. But a species which is rare compared to other, similar species will neither control the abundance of its resources, nor determine the abundance of its consumers. The population growth of a rare species does therefore not depend on its own density. On the long term, its population will either grow until it is not rare anymore, or the species will go extinct. Thus, the populations of all species are, on the log scale, near the upper limit in the population-dynamical steady state. In this context it is worth noting that, because the dynamics of rare species is linear, the precise value of the biomass at which species invade or go extinct (here chosen as  $B_i = M_i$ ) does not matter.

We now come back to the third question posed in the introduction and ask by which mechanism this upper limit, the equilibrium biomass, is determined. For the model, the following argument shows that this value must be determined bottom-up by the carrying capacity of producers. Since attack rates evolve freely, there are only two effects in the model that involve biomass density as parameters: one is the extinction of rare species at  $B_i = M_i$ , the other is the carrying capacity of producers  $B_i = K_i \sim M_i^{1/4}$  (see Appendix). But the extinction threshold does not affect equilibrium biomasses. This is suggested by the low density of species near the line  $B_i = M_i$  in Fig. 11 and the absence of such species in Fig. 13, and can be confirmed in numerical experiments varying the system size  $A$  (not shown). Producer carrying capacities are the only possible determinants of equilibrium biomass density remaining. Thus, while the biomass equilibrium is a top-down effect, the value of the equilibrium biomass density itself is controlled bottom-up.

Remarkably, time-averaged producer biomasses nevertheless remain about two orders of magnitude below their monoculture carrying capacity. We do not have a quantitative theory to predict this ratio, yet. Certainly, the strong regular or chaotic oscillations of producer biomasses (Fig. 5) are important: The maxima of these oscillations always have to remain below the carrying capacity, hence the mean values will be somewhat lower. But competition for resources between producers and consumption by herbivores will also play a role.

Taking the ratio between the monoculture carrying capacity of the smallest producers and typical mean biomasses actually reached into account by a correction factor  $C \approx 100$ , the equilibrium biomass is therefore given by  $B = K_p/C$ , where  $K_p$  is the carrying capacity for a small producer (e.g., phytoplankton) species in monoculture. The latter can be estimated as  $K_p = \text{GPP}_{\max}/\sigma_p$ , where  $\text{GPP}_{\max}$  is the gross primary production of monocultures, and  $\sigma_p$  is the maximum specific production rate of small producers. Thus, when the top-down mechanism is active, the prediction of the theory can be summarized by the following formula for typical abundances of species on the log scale:

$$N = \frac{\text{GPP}_{\max}}{C \sigma_p M}, \quad (1)$$

where  $N$  and  $M$  are the abundance and body mass of an arbitrary species at an arbitrary trophic level. We note that, apart from  $C$ , the right hand side of this formula contains only quantities related to the biology of individual species and the physical availability of the limiting resource, while the left hand side describes an aspect of ecology resulting from the interaction of many species. Predicting macroecological patterns based on general biological and physical facts is perhaps the most one can expect from a general macroecological theory.

## 6 Conclusions

Based on simulation results using a general multitrophic community model, we conclude that the top-down mechanism is a viable alternative to bottom-up mechanisms in controlling body mass –

abundance scaling. The top-down mechanism naturally leads to biomass densities independent of body mass, as they are frequently observed.

Since, in the model, the top-down mechanism operates at least partially on the evolutionary time scale, it might be difficult to identify it in the field. On population-dynamical time scales, one might simply find ecological parameters “magically” adjusted such as to yield constant biomass across trophic levels under bottom-up control. More research is necessary to better understanding the relative importance of evolutionary and population-dynamical contributions to the top-down mechanism.

Just as constant biomass is not always observed in nature, and many communities do show patterns compatible with the simple energetic equivalence rule, our model did not yield constant biomass for every parameter set considered. If, for example, parameters were chosen such that no or only few carnivores could evolve, we often observed a biomass dominance of large herbivores. We would therefore caution to conclude that the top-down mechanism is active in nature under all circumstances. But we believe that, in view of the ongoing debate and the unresolved issues surrounding body mass – abundance scaling, the idea deserves more attention.

### **Code and data availability**

Simulation code and data generated by the model is available from A.G.R..

### **Acknowledgements**

The authors express their gratitude Alan McKane and three anonymous reviewers for insightful comments on earlier versions of the paper, to Jennifer A. Dunne and Neo D. Martinez for making their food-web database available and to The 21st Century COE Program “Environmental Risk Management for Bio/Eco-Systems” of the Ministry of Education, Culture, Sports, Science and Technology of Japan for financial support. A.G.R. thanks the Frontier Research Center for Global Change for its hospitality.

### **Literature Cited**

- Amaral, L. A. N., Meyer, M., 1999. Environmental changes, coextinction, and patterns in the fossil record. *Phys. Rev. Lett.* 82 (3), 652–655.
- Banašek-Richter, C., Cattin, M.-F., Bersier, L.-F., 2005. Food web structure: from scale invariance to scale dependence and back again? In: de Ruiter, P., Wolters, V., Moore, J. C. (Eds.), *Dynamic food webs*. Academic Press, Amsterdam, Ch. 2.3, pp. 48–55.
- Benoît, E., Rochet, M.-J., 2004. A continuous model of biomass size spectra governed by predation and the effects of fishing on them. *J. Theor. Biol.* 226 (1), 9–21.
- Bersier, L.-F., Kehrli, P., 2007. The signature of phylogenetic constraints on food-web structure. *Ecological Complexity*, under review.
- Blackburn, T., Gaston, K., 1999. The relationship between animal abundance and body size: A review of mechanisms. *Advances in Ecological Research* 28, 181–210.
- Brose, U., Jonsson, T., Berlow, E. L., Warren, P., Banasek-Richter, C., Bersier, L.-F., Blanchard, J. L., Brey, T., Carpenter, S. R., Blandenier, M.-F. C., Cushing, L., Dawah, H. A., Dell, T., Edwards, F., Harper-Smith, S., Jacob, U., Ledger, M. E., Martinez, N. D., Memmott, J., Mintenbeck, K.,

- Pinnegar, J. K., Rall, B. C., Rayner, T. S., Reuman, D. C., Ruess, L., Ulrich, W., Williams, R. J., Woodward, G., Cohen, J. E., 2006. Consumer-resource body-size relationships in natural food webs. *Ecology* 87 (10), 2411–2417.
- Brown, J. H., Gillooly, J. F., Allen, A. P., Savage, V. M., West, G. B., 2004. Toward a metabolic theory of ecology. *Ecology* 85 (7), 1771–1789.
- Caldarelli, G., Higgs, P. G., McKane, A. J., 1998. Modelling coevolution in multispecies communities. *J. Theor. Biol.* 193, 345.
- Carbone, C., Gittleman, J. L., 2002. A common rule for the scaling of carnivore density. *Science* 295, 2273–2276.
- Christian, R. R., Luczkovich, J. J., 1999. Organizing and understanding a winter's seagrass foodweb network through effective trophic levels. *Ecological Modelling* 117, 99–124.
- Claessen, D., van Oss, C., Roos, A. M., Persson, L., 2002. The impact of size-dependent predation on population dynamics and individual life history. *Ecology* 83 (6), 1660–1675.
- Cohen, J. E., Briand, F., Newman, C. M., 1990. *Community Food Webs: Data and Theory*. Vol. 20 of *Biomathematics*. Springer, Berlin.
- Cohen, J. E., Jonsson, T., Carpenter, S. R., 2003. Ecological community description using the food web, species abundance, and body size. *PNAS* 100 (4), 1781–1786.
- Currie, D. J., 1993. What shape is the relationship between body size and population density? *Oikos* 66, 353–358.
- Cyr, H., 2000. The allometry of population density and inter-annual variability. In: Brown, J. H., West, G. B. (Eds.), *Scaling in biology*. Oxford University Press, Oxford, UK, pp. 267–295.
- Damuth, J., 1981. Population density and body size in mammals. *Nature* 290, 699–700.
- Damuth, J., 2007. A macroecological explanation for energy equivalence in the scaling of body size and population density. *Am. Nat.* 169 (5), 621–631.
- Drossel, B., Higgs, P. G., McKane, A. J., 2001. The influence of predator-prey population dynamics on the long-term evolution of food web structure. *J. Theor. Biol.* 208, 91–107.
- Drossel, B., McKane, A. J., Quince, C., 2004. The impact of nonlinear functional responses on the long-term evolution of food web structure. *J. Theor. Biol.* 229, 539–548.
- Duarte, C. M., Agusti, S., Peters, H., 1987. An upper limit to the abundance of aquatic organisms. *Oecologia* 74 (2), 272–276.
- Dunne, J. A., Williams, R. J., Martinez, N. D., Tiburon, R., 2002. Network structure and biodiversity loss in food webs: robustness increases with connectance. *Ecol. Lett.* 5 (4), 558.
- Gaedke, U., 1992. The size distribution of plankton biomass in a large lake and its seasonal variability. *Limnol. Oceanogr.* 37 (6), 1202–1220.

- Greenwood, J. J. D., Elton, R. A., 1979. Analysing experiments on frequency-dependent selection by predators. *J. Anim. Ecol.* 48, 721–737.
- Griffiths, D., 1992. Size, abundance, and energy use in communities. *J. Anim. Ecol.* 61, 307–315.
- Havlicek, T., Carpenter, S. R., 2001. Pelagic species size distributions in lakes: are they discontinuous? *Limnol. Oceanogr.* 46, 1021–1033.
- Jeschke, J. M., Kopp, M., Tollrian, R., 2004. Consumer-food systems: why type I functional responses are exclusive to filter feeders. *Biol. Rev.* 79, 337–349.
- Jonsson, T., Cohen, J. E., Carpenter, S. R., 2005. Food webs, body size, and species abundance in ecological community description. *Adv. Ecol. Res.* 36, 1–84.
- Levine, S., 1980. Several measures of trophic structure applied to complex food webs. *J. Theor. Biol.* 83, 195–207.
- Li, B.-L., Gorshkov, V. G., Makarieva, A. M., 2004. Energy partitioning between different-sized organisms and ecosystem stability. *Ecology* 85 (7), 1811–1813.
- Loeuille, N., Loreau, M., 2005. Evolutionary emergence of size-structured food webs. *PNAS* 102 (16), 5761–5766.
- Loeuille, N., Loreau, M., 2006. Evolution of body size in food webs: does the energetic equivalence rule hold? *Ecology Letters* 9, 171–178.
- Marquet, P. A., 2002. Of predators, prey, and power laws. *Science* 295, 2229–2230.
- Marquet, P. A., Navarrete, S. A., Castilla, J. C., 1995. Body size, population density, and the energetic equivalence rule. *J. Anim. Ecol.* 64, 325–332.
- Marquet, P. A., Quiñones, R. A., Abades, S., Labra, F., Tognelli, M., 2005. Scaling and power-laws in ecological systems. *J. Exp. Biol.* 208, 1749–1769.
- May, R. M., 1972. Will a large complex system be stable? *Nature* 238, 413–414.
- McNiel, S., Lawton, J. H., 1970. Annual production and respiration in animal populations. *Nature* 225, 472–474.
- Meehan, T. D., 2006. Energy use and animal abundance in litter and soil communities. *Ecology* 87 (7), 1650–1658.
- Mulder, C., Cohen, J. E., Setälä, H., Bloem, J., Breure, A. M., 2005. Bacterial traits, organism mass, and numerical abundance in the detrital soil food web of dutch agricultural grasslands. *Ecology Letters* 8, 80–90.
- Nee, S., Read, A. F., Greenwood, J., Harvey, P., 1991. The relationship between abundance and body size in British birds. *Nature* 351, 312–313.
- Oaten, A., Murdoch, W., 1975. Switching, functional response, and stability in predator-prey systems. *American Naturalist* 109 (967), 299–318.

- Peters, R. H., 1983. The ecological implications of body size. Cambridge University Press, Cambridge.
- Platt, T., Denman, K., 1977. Organization in the pelagic ecosystem. *Helgol. Wiss. Meeresunters.* 30, 575–581.
- Platt, T., Denman, K., 1978. The structure of pelagic ecosystems. *Rapp. P-V. Reun. Cons. Int. Explor. Mer.* 173, 60–65.
- Quiñones, R. A., Platt, T., Rodríguez, J., 2003. Patterns of biomass-size spectra from oligotrophic waters of the Northwest Atlantic. *Progr. Oceanog.* 57, 405–427.
- Rodriguez, J., Mullin, M., 1986. Relation between biomass and body weight of plankton in a steady state oceanic ecosystem. *Limnol. Oceanog.* 31, 361–370.
- Rossberg, A. G., 2007. Part-whole relations between food webs and the validity of local food-web descriptions. *Ecological Complexity* Accepted.
- Rossberg, A. G., Matsuda, H., Amemiya, T., Itoh, K., 2006a. Food webs: Experts consuming families of experts. *J. Theor. Biol.* 241 (3), 552–563.
- Rossberg, A. G., Yanagi, K., Amemiya, T., Itoh, K., 2006b. Estimating trophic link density from quantitative but incomplete diet data. *J. Theor. Biol.* 243 (2), 261–272.
- Savage, V. M., Gillooly, J. F., Brown, J. H., West, G. B., Charnov, E. L., 2004. Effects of body size and temperature on population growth. *Am. Nat.* 163 (3), 429–441.
- Sheldon, R. W., Prakash, A., W. H. Sutcliffe, J., 1972. The size distribution of particles in the ocean. *Limnol. Oceanogr.* 17, 327–340.
- Solé, R. V., Manrubia, S. C., Benton, M., Bak, P., 1997. Self-similarity of extinction statistics in the fossil record. *Nature* 388, 764–767.
- Sprules, W. G., Munawar, M., 1986. Plankton size spectra in relation to ecosystem productivity, size, and perturbation. *Canadian Journal of Fisheries and Aquatic Science* 43, 1789–1794.
- Whittaker, R. H., 1965. Dominance and diversity in plant communities. *Science* 147, 250–260.
- Williams, R. J., Martinez, N. D., 2000. Simple rules yield complex food webs. *Nature* 404, 180–183.
- Yoshida, K., 2003. Dynamics of evolutionary patterns of clades in a food web system model. *Ecological Research* 18, 625–637.

## Appendix: Model Details

In the following, we give a compact technical definition of the full model, suitable for writing a numerical simulation code. The parametrization and the motivations and implications of design decisions are discussed in Section A2. Table A1 lists model parameters and variables.

### A1 Model Definition

#### A1.1 Model states

Each consumer species  $i$  is characterized by its mean body mass  $M_i$  ( $M_{\min} \leq M_i \leq M_{\max}$ ), its current total biomass  $B_i(t)$ , a  $D$ -dimensional vector of abstract quantitative vulnerability traits  $\vec{V}_i$ , another  $D$  dimensional vector  $\vec{F}_i$  describing foraging traits and capabilities, its attack rate  $a_i$ , and a switching exponent  $b_i$ . Producer species  $i$  are characterized by  $M_i$ ,  $B_i(t)$ ,  $\vec{V}_i$ , and a  $D$ -dimensional vector  $\vec{G}_i$  describing the non-trophic producer niche.

A community is fully characterized by its constituent consumers and producers. The complete model state consists of four communities.

#### A1.2 Population dynamics

Consumer population dynamics is of the standard form

$$\frac{dB_i}{dt} = \underbrace{\epsilon \sum_{\text{species } k} f_{ki} B_i}_{\text{eating}} - \underbrace{\sum_{\text{consumers } l} f_{li} B_l}_{\text{being eaten}} - \underbrace{r_i B_i}_{\text{respiration}}. \quad (\text{A1})$$

The functional response  $f_{ki}$  has been constructed in such a way as to satisfy three conditions. If there is only a single resource species or if all resource abundances are scaled by the same factor, the standard Type II form should be recovered, because Type II responses are overwhelmingly observed (Jeschke et al., 2004). If, on the other hand, resource abundances vary disproportionally, the relative intake should follow the power-law form  $f_{ki}/f_{li} \sim (B_k/B_l)^{b_i}$  which is found in experiments (e.g., Greenwood and Elton, 1979; Elliott, 2004). Finally the biomasses of species not contributing to the diet should not affect the functional response. These conditions are satisfied by

$$f_{ki} = \frac{a_i (c_{ki} B_k)^{b_i}}{\beta_i^{b_i-1} + T_i a_i \sum_j (c_{ji} B_j)^{b_i}} \text{ with } \log \beta_i = \frac{\sum_j c_{ji} B_j \log c_{ji} B_j}{\sum_j c_{ji} B_j}, \quad (\text{A2})$$

with  $a_i$  and  $T_i$  representing the attack rate and the “handling time” of consumer  $i$ , and the  $c_{ki}$  denoting trophic interaction coefficients.

However, this form fails to satisfy a “common sense” condition pointed out by Arditi and Michalski (1995) and Berryman et al. (1995): Dynamics is not invariant if a resource population is formally split into two populations with identical traits.

This problem can be overcome by organizing resources  $k$  into groups  $\gamma = \Gamma(k)$  of similar species, within which consumers cannot distinguish when switching prey. Among group members, consumers forage proportional to the resource availability  $c_{ki} B_k$ . The groups are formed, for simplicity, by dividing the  $D$ -dimensional trophic niche space into a lattice of cells with lattice constant  $u$ , and assigning all species with a vulnerability  $\vec{V}_k$  in the same cell to the same group. Denote by  $A_{\gamma i} =$

$\sum_{\Gamma(k)=\gamma} c_{ki} B_k$  the total availability of resource species in group  $\gamma$  to consumer  $i$ . Then, a second, “common sense”, form of the functional response is given by

$$f_{ki} = \frac{c_{ki} B_k}{A_{\Gamma(k)i}} \cdot \frac{a_i A_{\Gamma(k)i}^{b_i}}{\beta_i^{b_i-1} + T_i a_i \sum_{\gamma} A_{\gamma i}^{b_i}} \text{ with } \log \beta_i = \frac{\sum_{\gamma} A_{\gamma i} \log A_{\gamma i}}{\sum_{\gamma} A_{\gamma i}}. \quad (\text{A3})$$

When no two  $\vec{V}_k$  are identical, which is practically always the case with the evolutionary dynamics given below, the second form of the functional response goes over into the first form (A2) in the limit of small cells  $u \rightarrow 0$ .

The trophic interaction coefficients are composed as

$$c_{ki} = \overbrace{\exp\left[-\frac{|\vec{V}_k - \vec{F}_i|^2}{2 w_t^2}\right]}^{\text{trophic trait matching}} \times \overbrace{\left(\frac{M_k}{M_i}\right)^{\alpha}}^{\text{small resource cutoff}} \times \overbrace{\begin{cases} \exp(-\Lambda M_k/M_i) & \text{for consumer } k, \\ 1 & \text{for producer } k, \end{cases}}^{\text{large resource cutoff}} \quad (\text{A4})$$

where the form of the last two factors follows Claessen et al. (2002).

Producer population dynamics is modeled as

$$\frac{dB_i}{dt} = \overbrace{\sigma_i \exp\left(-\sum_{\text{producers } j} d_{ij} B_j\right)}^{\text{competition, resource exploitation}} B_i - \overbrace{\sum_{\text{consumers } k} f_{ik} B_k}^{\text{being eaten}} - \overbrace{l_i B_i}^{\text{losses}}, \quad (\text{A5})$$

The exponential form of the factor describing the availability of resources in the first term is inspired by the attenuation of light (Monsi and Saeki, 1953), but it could describe the depletion of other resources as well.

The matrix  $d_{ij}$  describes producer competition and self-interaction. Mutualistic and parasitic producer-producer interactions are not included in the model. The niche overlap between two producer species  $i, j$  is modeled as  $\exp[-|\vec{G}_i - \vec{G}_j|^2/2w_r^2]$ , with  $w_r$  denoting the producer niche width. This leads to the resource competition matrix

$$d_{ij} = d_{jj} \overbrace{\exp\left[-\frac{|\vec{G}_i - \vec{G}_j|^2}{2 w_r^2}\right]}^{\text{producer niche overlap}}. \quad (\text{A6})$$

The species-specific coefficients follow allometric scaling laws  $d_{jj}, l_j \sim M_j^{\zeta}$  and  $r_j, T_j^{-1} \sim M_j^{\zeta_r}$ , with  $\zeta = \zeta_r = -1/4$  in the standard case.

### A1.3 Species evolution

Next, we describe the implementations of “speciations” and “invasions” in the model. As explained in Sec. 2.2 of the main text, these are extremely coarse-grained descriptions of the actual evolutionary processes. To model a “speciation”, the properties of a descendant species  $j$  are obtained by mutating the properties of its ancestor  $i$ . The biomass of the descendant species is given by

$$M_j = d^{\xi} M_i \quad (\text{A7})$$

with  $\xi$  denoting a standard-normal random variable, newly sampled at each use. If  $M_j$  falls outside the range  $[M_{\min}, M_{\max}]$ , it is projected back into this range by the operations  $M_j \rightarrow M_{\min}^2/M_j$  or  $M_j \rightarrow M_{\max}^2/M_j$ , which correspond to simple reflections on the log scale (Rossberg et al., 2006). Traits mutate as

$$\vec{V}_j = \frac{(\vec{V}_i - \vec{V}_j^0) + \mu_V \vec{\xi}}{\sqrt{1 + \mu_V^2/\sigma_V^2}} + \vec{V}_j^0, \quad (\text{A8})$$

$$\vec{F}_j = \frac{\vec{F}_i + \mu_F \vec{\xi}}{\sqrt{1 + \mu_F^2/\sigma_F^2}}, \quad (\text{A9})$$

$$\vec{G}_j = \frac{\vec{G}_i + \mu_G \vec{\xi}}{\sqrt{1 + \mu_G^2/\sigma_G^2}}, \quad (\text{A10})$$

with  $\vec{V}_j^0 = (s_j, 0, 0, 0, 0)$ ,  $s_j = s/2$  for producers and  $s_j = -s/2$  for consumers, to model the distinct characteristics of the members of the two kingdoms as resources. The  $\vec{\xi}$  denote standard normal random vectors, the  $\mu$ s and  $\sigma$ s are model parameters.

The attack rate of the descendant species is given by

$$a_j = \left(\frac{M_j}{M_i}\right)^\zeta \times a_0 \times \tilde{a}_0^\xi \times a_i \quad (\text{A11})$$

This inheritance rule has the following interpretation: The first factor implies a background allometric scaling of attack rates with body mass,  $a_i \sim M_i^\zeta$ , the second factor, with  $0 < a_0 < 1$ , describes a degeneration of aggressivity in the absence of evolutionary pressures, and the third factor contributes a random mutation. Equation (A11) is set up to be scale free in the sense that it does not imply a typical order of magnitude for the attack rates  $a_i$  or the allometric coefficients  $a_i (M_i/M_0)^{-\zeta}$ . This follows from the fact that all three parameters  $\zeta$ ,  $a_0$ ,  $\tilde{a}_0$  in Eq. (A11) are dimensionless, while the  $a_i$  have dimensions of  $(\text{time} \times \text{biomass})^{-1}$ .

The heredity of switching exponents is assumed to be negligibly small. Thus  $b_j$  is simply given by

$$b_j = b_0 + \tilde{b}_0 \xi \quad (\text{A12})$$

with constant  $b_0$  and  $\tilde{b}_0$ .

Except for the attack rates, this model of speciation implies a simple neutral theory: In the steady-state distribution resulting from speciations as above and random extinctions, log body masses are distributed uniformly in  $[\log M_{\min}, \log M_{\max}]$ , and trait vectors are given by

$$\vec{V}_i = \sigma_V \vec{\xi} + \vec{V}_i^0, \quad \vec{F}_i = \sigma_F \vec{\xi}, \quad \vec{G}_i = \sigma_G \vec{\xi}. \quad (\text{A13})$$

To model the “invasion” of species, two pools of representative species are assembled from the other three communities as described below, one for producers and one for consumers. The properties of an invading species are obtained by picking one species from the pool at random, and mutating it in the same way as for speciations. The additional mutation represents evolutionary changes occurring in the surrounding, not explicitly modeled, communities (Fig. 1).

If a species pool is empty, which happens only in the initial phase of the simulation with the parameters used here, an invading species is sampled from the steady state of the neutral theory, with the attack rate set to  $a_i = a_{\text{start}}(M_i/M_0)^\zeta$  with constant  $a_{\text{start}}$ .

Initial biomasses  $B_j$  of speciating or invading species are set to  $M_j$ .

#### A1.4 Community evolution

The community evolves by repeated additions (successful speciations or invasions) of a producer and a consumers species and the subsequent relaxations to the population-dynamical steady state. If a species reaches  $B_i < M_i$  during the relaxation, it is removed as extinct. A speciation or invasion is successful (and hence an addition) if its population initially grows ( $dB/dt > 0$ ). Speciation and invasions are repeatedly attempted until successful<sup>3</sup>. At each repetition, the attempted addition is an invasion with probability  $\kappa/(\kappa + S_p)$ , where  $S_p$  denotes the producer species abundance, and otherwise a speciation from a producer species chosen randomly from the local community. Correspondingly for additions of consumers.

Simulations are initiated with four empty communities and run until an evolutionary steady state is reached.

#### A1.5 Construction of representative species pools

Representative species pools for invasions of communities by producers are constructed by combining all producer species from the other three modeled communities, and correspondingly for consumers. To reduce waiting times when parallelizing the simulations, the information about the species compositions of the other communities is updated only after every 30 additions of one consumer and one producer, i.e., a total of 60 s.a., into each of the four communities.

#### A1.6 Numerical implementation

With body masses spanning 12 to 14 orders of magnitudes, and the corresponding time scales spanning tree to four, special care was required with the numerical implementation of the population-dynamical sub-model. For a stable, accurate, and fast numerical integration, the population-dynamic equations (A1) and (A5) were first transformed to new dependent variables  $\hat{B}(t) = \ln B(t)$ , and then integrated using the adaptive-order, adaptive-stepsize, implicit ODE solver CVODE included in the SUNDIALS package (Hindmarsh et al., 2005).

In order to approach the population-dynamical steady state, simulations were continued until either limit-cycle oscillations or chaotic oscillations were detected using heuristic algorithms, or until a long time  $T_{SS}$  had passed without detecting either, which usually indicates the vicinity of a fixed point. As mentioned above, species  $i$  with  $B_i < M_i$  were removed as locally extinct during simulations.

The four communities were simulated on separate processors. After every 60 s.a. in each community and the subsequent population-dynamical relaxation to the steady state, the full model state was saved for an update of species pools among communities (see Sec. A1.5) and for later data analysis.

<sup>3</sup>In about 2% of all cases, no species with positive growth rate can be found for a given population-dynamical state, even after 1000 attempts. In order to avoid blocking the simulations, the condition  $dB/dt > 0$  is then dropped, and the addition is counted as “successful”, even though the inserted species will immediately go extinct.

## A2 Model design and parameter choices

In this Appendix, the rational behind several aspects of model design and parameter choices is explained. It begins with a discussion of two aspects of niche-space structure: phylogenetic correlations of trophic traits and the number of dimensions of the niche space. Then, the parametrization and allometry of consumer and producer population dynamics is derived from empirical data; followed by a brief account of the parametrization of other aspects of trophic interaction. For some aspects of the model, most of them related to the geometry of niche space, satisfactory empirical data do not seem to be available. These have been adjusted “by hand” following the criteria discussed at the end of this Appendix.

### A2.1 Phylogenetic correlations

The starting point for constructing the present model was the matching model (Rossberg et al., 2006). In the matching model, food webs are constructed by a branching process that models the evolution of the member species. It is a neutral theory, in the sense that evolution is undirected, independent of the fitness or population dynamics of species. Trophic links are determined by matching abstract traits determining the vulnerabilities of potential resources to consumption with abstract traits determining the foraging capabilities and strategies of consumers.

Fitting the matching model to empirical data, Rossberg et al. (2006) found that the heredity of vulnerability traits in local “speciations” (*sensu* Sec. 2.2) is considerably larger than of foraging traits: the median (average) of the decay rate of correlations in the vulnerability traits over all predatory food webs investigated is 1.4% per “speciation” (1.8%), while correlations between foraging traits decay by 22% per “speciation” (36%). This observation was interpreted as indicating that the evolutionary pressure through competition for resources is stronger than the pressure through indirect competition due to common predators. L.-F. Bersier (priv. comm.) suggested an alternative interpretation, which is employed in the present model: Foraging traits are simply more easily adjustable than vulnerability traits, and have higher variability.

In the neural theory for the present model, the correlation-decay rate of vulnerability traits  $\vec{V}_i$  is  $1 - (1 + \mu_V^2/\sigma_V^2)^{-1/2} \approx \mu_V^2/2\sigma_V^2$  per speciation, where  $\mu_V$  is the magnitude of typical mutations in speciations, and  $\sigma_V$  is the steady-state variability of traits. (Similar results hold for foraging traits  $\vec{F}_i$  and producer-interaction traits  $\vec{G}_i$ .) However, in the presence of evolutionary pressures, both the magnitude of mutations and the steady-state variability for the  $\vec{V}_i$  will increase, and the variability of foraging traits is restricted to the variability of the corresponding vulnerability traits, and all these quantities are difficult to predict in advance. Thus, reproducing the observed patterns of trait correlations quantitatively is not easy. Yet, in order to stay in line with observations, parameters were chosen such as to keep the decay of correlations of foraging traits large,  $(\mu_F/\sigma_F)^2 = \mathcal{O}(1)$ , and the decay of correlations of vulnerability traits small,  $(\mu_V/\sigma_V)^2 = \mathcal{O}(1\%)$ . Regarding the correlations of  $\vec{G}_i$  in speciations, no empirical data could be obtained.

### A2.2 Dimensionality of niche space

For the matching model, it has been argued that the dimensionality of the trophic niche space does not matter much, as long as it is not too small (Rossberg et al., 2006). An important effect of high dimensionality  $D$ , i.e., of many relevant traits, is that different consumers are likely to consume the same resources for different reasons (Rossberg, 2007): Consider the situation that two consumers 1

and 2 have foraging traits  $\vec{F}_1$  and  $\vec{F}_2$  that are both close to the vulnerability traits  $\vec{V}_3$  of resource 3, such that the factor  $e_{ki} := \exp(-|\vec{V}_k - \vec{F}_i|^2/2w_t^2)$  entering the interaction coefficients Eq. (A4) is comparatively large (an exact match is very unlikely). Then, if  $\vec{F}_1$  is also close to another, unrelated  $\vec{V}_4$ , this does not imply that  $\vec{F}_2$  is likely to be close to  $\vec{V}_4$ , too, if the number of dimensions is large. This is because then  $\vec{F}_1$  and  $\vec{F}_2$  are likely to approach  $\vec{V}_3$  from different directions. Mathematically, the relevant quantity is the correlation  $\rho_D$  between the two products  $e_{3,1} \times e_{3,2}$  and  $e_{4,1} \times e_{4,2}$ . When evaluating this correlation numerically, for example, with independent,  $D$ -dimensional, multivariate standard normal  $\vec{F}_1$ ,  $\vec{F}_2$ ,  $\vec{V}_3$ , and  $\vec{V}_4$  and the niche width  $w_t = 0.446$  (Tab. A1), one obtains  $\rho_1 = 0.25$ ,  $\rho_2 = 0.16$ ,  $\rho_3 = 0.096$ ,  $\rho_4 = 0.055$ , and  $\rho_5 = 0.030$ . The correlations decay exponentially, roughly by a factor 0.6 with each additional dimension.

We find that the standard error in estimating  $\rho_5$  from  $N$  independent quadruples of samples is approximately  $\rho_5 \times 150 N^{-1/2}$ , that is, detecting that  $\rho_5 \neq 0$  requires about  $(2 \times 150)^2 = 90000$  independent quadruples. Since typical model food webs consist only of  $\sim 100$  species, and these are phylogenetically correlated, it is fair to assume that when choosing  $D = 5$  the phylogenetic correlation structure underlying food-web topology is hardly distinguishable from that with any larger number of dimensions in the model. Here,  $D = 5$  is used. With an even larger number of dimensions, the volume of the accessible niche space, which scales as the variability of vulnerability traits to the  $D$ th power, and, as a result, the number of species, would be difficult to control.<sup>4</sup>

### A2.3 Consumer physiology

Consumer population dynamics is characterized by the gross conversion efficiency  $\epsilon$ , respiration rates  $r_i$ , “handling times”  $T_k$ , attack rates  $a_k$ , and the trophic interaction coefficients.

To determine the first three parameters, consider a situation of abundant resources (*ad libitum* feeding) for species  $i$ . Then, for both forms of the functional response (A2), (A3), the summed functional response reduce to  $\sum_l f_{li} = 1/T_i$  and, in the absence of predation, population  $i$  increases at its maximal growth rate  $r_{\max,i} = \epsilon/T_i - r_i$ .

While producing biomass at a rate  $P = (\epsilon/T_i - r_i)B_i$ , species  $i$  is, by the passive consumption terms of Eqs. (A1) and (A5) summed over all resource species, consuming biomass at a rate  $B_i/T_i$ . Thus, the net conversion efficiency is  $\epsilon_0 = \epsilon - r_i T_i$ . We set  $\epsilon_0 = 0.2$ , a typical empirical value for poikilotherms (Peters, 1983).

The term  $-r_i B_i$  in Eq. (A1) represents all losses other than by passive consumption. Usually, this will be dominated by respiration, losses by natural death are negligibly small.<sup>5</sup> Observed values for the ratio  $P/R$  of production to respiration vary from  $\sim 10$  or higher for bacteria to  $\sim 0.01$  for homeotherms (McNiel and Lawton, 1970). We use the value found by McNiel and Lawton for “short-lived poikilotherms”,  $P/R = 0.8$ . Altogether, these considerations lead to

$$\epsilon = \left(1 + \frac{R}{P}\right) \epsilon_0, \quad T_i = \frac{\epsilon_0}{r_{\max,i}}, \quad r_i = \frac{R}{P} r_{\max,i}. \quad (\text{A14})$$

The maximum consumer population growth rate  $r_{\max,i}$  is known to follow an allometric scaling law. Based on the result of Savage et al. (2004) for intermediate temperatures, we set  $r_{\max,i} = 0.81 \text{ yr}^{-1} (M_i/M_0)^{\zeta_r}$ , with  $\zeta_r = -1/4$ .

<sup>4</sup>For the neutral matching model (Rossberg et al., 2006) a much higher number of traits is used in order to reduce discretization effects, since, contrary to the situation here, the matched traits are binary (yes/no). The number of species in this model does not depend on niche-space geometry.

<sup>5</sup>Since the model does not describe birth or death of individuals, effects of demographic stochasticity are not included. They would have little effect on the results, since most populations are large (Fig. 12).

In correspondence with the range of switching exponents obtained by Greenwood and Elton (1979) in a re-analysis of 14 laboratory experiments, we set the mean switching exponent to  $b_0 = 1.5$  and its standard deviation to  $\tilde{b}_0 = 0.3$ . Field data on prey switching still seem to be rare (Elliott, 2004).

## A2.4 Producer physiology and interaction

The model for producer population dynamics Eq. (A5) implies a maximal population growth rate for producers  $\sigma_{\max,i} = \sigma_i - l_i$ , which is set to  $\sigma_{\max,i} = \sigma_{\max,0} (M_i/M_0)^{-1/4}$  with  $\sigma_{\max,0} = 0.208 \text{ year}^{-1}$  after Niklas and Enquist (2001). The ratio between the maximum growth rate  $\sigma_i - l_i$  and the respiration rate  $l_i$  was set to  $(\sigma_i - l_i)/l_i = (1 - 0.1)/0.1 = 9$  as a plausible value.<sup>6</sup>

To determine the diagonal elements of the resource competition matrix  $d_{ij}$ , Eq. (A6), we make use of the fact that the maximal production of producers at their carrying capacity  $B_i = K_i$  is uncorrelated to their body mass (Enquist et al., 1998). Therefore, carrying capacities are chosen such that the maximal gross primary production defined by  $\text{GPP}_{\max} = \sigma_i K_i$  is constant. (Since the losses described by the factors  $l_i$  include both respiration and litter fall, the model does not define the net primary production.) As a convention,  $\text{GPP}_{\max}$  and the  $K_i$  are here understood as extensive quantities, that is, they are proportional to the area  $A$  covered by each of the modeled communities. By Eq. (A5), the carrying capacity of monocultures of producers is  $K_i = (1/d_{ii}) \log(\sigma_i/l_i)$ , which, in turn, determines the diagonal elements of the competition matrix as

$$d_{ii} = \sigma_i \frac{\log(\sigma_i/l_i)}{\text{GPP}_{\max}}. \quad (\text{A15})$$

## A2.5 Other aspects of trophic interaction

Prey switching facilitates coexistence in the model, especially between producers. In particular, we found that with the first form for the functional response, or the second form with  $u \rightarrow 0$ , which imply switching between any pair of resources, communities sometimes fall into unrealistic “gardening” states where a few tens of herbivores mediate coexistence of thousands of producers. With our choice  $u = 1$  such states are not observed. Further disabling switching by increasing  $u$  would strongly reduce the number of coexisting species.

A value of  $\Lambda \approx 0.03$  for the lower cutoff for the predator-prey size ratio is suggested by the evaluation of a large set of empirical data by Brose et al. (2006). The extension of the body mass range occupied by consumers sensitively depends on the exponent  $\alpha$  that characterizes the decay of cacheability with large predator-prey mass ratios. With  $\alpha = 0$ , arbitrary large body sizes up to  $M_{\max}$  are observed. With the parameter set used here, the choice  $\alpha = 0.075$  restricts body masses to approximately 10 kg.

## A2.6 Model calibration

The reader will notice that some of the parameters listed in Tab. A1 have rather odd values, even though they are not directly based on empirical data. There are several reasons.

First, the way in which the parameter space is spanned in the computer model is slightly different from the way chosen here. For example, trophic niche widths had been expressed in terms of trophic niche densities  $\sim w_t^{-D}, w_r^{-D}$ , but this would here only confound notation.

<sup>6</sup> This ratio should not be confused with the ratio of producer production to respiration in the steady state, which is routinely measured.

Second, some parameter calibration is required in order to obtain a reasonable community structure in the steady state. It was attempted (i) to keep the numbers of producer and consumer species similar; (ii) to make sure that some consumers are omnivores *sensu stricto*, eating producers and consumers alike, while others are not (this can be achieved by controlling the ranges of vulnerability traits covered by producers and consumers in trophic niche space); (iii) to keep the fraction of top-predators around 0.2 as observed, (iv) to obtain a large number of trophic links per consumer, and (v) to have consumers cover a broad range of body masses, but to avoid producing a Loch Ness Monster or hitting  $M_{\max}$ .

Third, the computation time required to reach the steady state increases at least with the square of the number of species simulated. Simulations of systems with about 100 species per community take several days to reach the steady state. On the other hand, a large number of species is desired in order to reproduce collective, system-level ecological phenomena. Therefore, the steady-state number of species must be controlled in a narrow range. But the number of species appears to depend on most system parameters in a complicated way, and initial transients provide only little clues where it will ultimately settle in. Adjusting one parameter usually requires adjusting a second one in order to keep the number of species fixed, and the outcome is not always predictable.

Fourth, some parameter values were found to yield reasonable results at an earlier stage of model development, and were later kept fixed for simplicity.

Summarizing, much effort has been made to calibrate the model such as to obtain reasonable community structures within the computational limitations. The rationale was that the demonstration of the top-down mechanism in a model that exhibits strong artifacts would not exclude the possibility that these artifacts were required for the mechanism to work. But in fact, rather the contrary seems to be true: Observations during the model calibration indicate that the requirements on parameters for the top-down mechanism to work are less restrictive than the requirement for achieving all the other community properties listed above.

## References

- Arditi, R., Michalski, J., 1995. Nonlinear food web models and their responses to increased basal productivity. In: Polis, G. A., Winemiller, K. O. (Eds.), *Integration of Patterns and Dynamics*. Chapman & Hall, London, pp. 122–133.
- Berryman, A. A., Michalski, J., Gutierrez, A. P., Arditi, R., 1995. Logistic theory of food web dynamics. *Ecology* 76, 336–343.
- Brose, U., Jonsson, T., Berlow, E. L., Warren, P., Banasek-Richter, C., Bersier, L.-F., Blanchard, J. L., Brey, T., Carpenter, S. R., Blandenier, M.-F. C., Cushing, L., Dawah, H. A., Dell, T., Edwards, F., Harper-Smith, S., Jacob, U., Ledger, M. E., Martinez, N. D., Memmott, J., Mintenbeck, K., Pinnegar, J. K., Rall, B. C., Rayner, T. S., Reuman, D. C., Ruess, L., Ulrich, W., Williams, R. J., Woodward, G., Cohen, J. E., 2006. Consumer-resource body-size relationships in natural food webs. *Ecology* 87 (10), 2411–2417.
- Claessen, D., van Oss, C., Roos, A. M., Persson, L., 2002. The impact of size-dependent predation on population dynamics and individual life history. *Ecology* 83 (6), 1660–1675.
- Elliott, J. M., 2004. Prey switching in four species of carnivorous stoneflies. *Freshwater Biology* 49, 709–729.

- Enquist, B. J., Brown, J. H., West, G. B., 1998. Allometric scaling of plant energetics and population density. *Nature* 395, 163–165.
- Greenwood, J. J. D., Elton, R. A., 1979. Analysing experiments on frequency-dependent selection by predators. *J. Anim. Ecol.* 48, 721–737.
- Hindmarsh, A. C., Brown, P. N., Grant, K. E., Lee, S. L., Serban, R., Shumaker, D. E., Woodward, C. S., 2005. SUNDIALS: Suite of Nonlinear and Differential/Algebraic Equation Solvers. *ACM Trans. Math. Soft.* 31 (3), 363–396.
- Jeschke, J. M., Kopp, M., Tollrian, R., 2004. Consumer-food systems: why type I functional responses are exclusive to filter feeders. *Biol. Rev.* 79, 337–349.
- McNiel, S., Lawton, J. H., 1970. Annual production and respiration in animal populations. *Nature* 225, 472–474.
- Monsi, M., Saeki, T., 1953. Über den Lichtfaktor in den Pflanzengesellschaften und seine Bedeutung für die Stoffproduktion. *Japanese Journal of Botany* 14, 22–52.
- Niklas, K. J., Enquist, B. J., 2001. Invariant scaling relationships for interspecific plant biomass production rates and body size. *PNAS* 98 (5), 2922–2927.
- Peters, R. H., 1983. The ecological implications of body size. Cambridge University Press, Cambridge.
- Rossberg, A. G., 2007. Part-whole relations between food webs and the validity of local food-web descriptions. *Ecological Complexity* Accepted.
- Rossberg, A. G., Matsuda, H., Amemiya, T., Itoh, K., 2006. Food webs: Experts consuming families of experts. *J. Theor. Biol.* 241 (3), 552–563.
- Savage, V. M., Gillooly, J. F., Brown, J. H., West, G. B., Charnov, E. L., 2004. Effects of body size and temperature on population growth. *Am. Nat.* 163 (3), 429–441.

Table A1: Model parameters and state variables

Symbol	Description	Important Equations	Range or Standard Value
$A$	system area		1000 ha
$M_i$	body mass of species $i$	A7	$M_{\min} \leq M_i \leq M_{\max}$
$M_{\min}$	smallest allowed body mass	A7	$10^{-13}$ kg
$M_{\max}$	largest allowed body mass	A7	$10^3$ kg
$d$	variation of body mass in speciations	A7	3.0
$M_0$	allometric base unit		1 kg
$B_i$	biomass of species $i$	A1,A5	$B_i \geq M_i$
$\zeta$	general allometric exponent		-1/4
$\zeta_r$	allometric exponent consumer metabolism		-1/4
$T_i$	resource “handling” time of consumer $i$	A2,A3,A14	$T_i > 0$
$a_i$	attack rate of consumer $i$	A2,A3,A11	$a_i > 0$
$a_0$	degeneration of attack rates in speciations	A11	0.9
$\tilde{a}_0$	variation of attack rates in speciations	A11	1.2
$a_{\text{start}}$	attack rate initializer	Sec. A1.5	$10^7 \text{ m}^2 \text{ kg}^{-1} \text{ yr}^{-1} / A$
$b_i$	switching exponent of consumer $i$	A2,A3,A12	see below
$b_0$	mean switching exponent	A12	1.5
$\tilde{b}_0$	std switching exponent	A12	0.3
$u$	resolution of resources when switching	A3	1
$\epsilon$	gross conversion efficiency	A1,A14	0.45
$\epsilon_0$	net conversion efficiency	A14	0.2
$P/R$	consumer production/respiration ratio	A14	0.8
$r_i$	respiration rate of consumer $i$	A1,A14	$r_i > 0$
$c_{ki}$	trophic interaction coefficients	A2,A3,A4	$c_{ki} > 0$
$w_t$	trophic niche width	A4	0.446
$\alpha$	small resource cutoff exponent	A4	0.075
$\Lambda$	min predator-prey mean body mass ratio	A4	0.03
$r_{\max,i}$	max population growth rate of consumer $i$	A14	$0.81 \text{ yr}^{-1} (M_i/M_0)^{\zeta_r}$
$\text{GPP}_{\max}$	monoculture GPP	A15	$10^3 \text{ kg yr}^{-1} \text{ m}^{-2} \times A$
$\sigma_{\max,i}$	max population growth rate of producer $i$	Sec. A2.4	$0.208 \text{ yr}^{-1} (M_i/M_0)^{-1/4}$
$l_i$	loss rate of producer $i$	A5	$\sigma_{\max,i}/9$
$\sigma_i$	gross population growth rate of producer $i$	A5	$\sigma_{\max,i} + l_i$
$d_{ij}$	producer resource competition matrix	A6	$d_{ij} > 0$
$w_r$	producer niche width	A6	0.976
$T_{\text{SS}}$	max population-dynamical relaxation time	Sec. A1.6	30 yr
$D$	dimensionality of niche spaces	Sec. A2.2	5
$\vec{V}_i$	vulnerability traits of species $i$	A8	$\vec{V}_i \in \mathbf{R}^D$

Symbol	Description	Important Equations	Range or Standard Value
$\vec{F}_i$	foraging traits of consumer $i$	A9	$\vec{F}_i \in \mathbf{R}^D$
$\vec{G}_i$	niche traits of producer $i$	A10	$\vec{G}_i \in \mathbf{R}^D$
$s$	producer-consumer trait separation	A8	1.4
$\sigma_V$	nominal variability of $\vec{V}_i$	A8	0.2
$\sigma_F$	nominal variability of $\vec{F}_i$	A9	3.0
$\sigma_G$	nominal variability of $\vec{G}_i$	A10	1.0
$\mu_V$	mutation of $\vec{V}_i$ in speciations	A8	0.025
$\mu_F$	mutation of $\vec{F}_i$ in speciations	A9	6.0
$\mu_G$	mutation of $\vec{G}_i$ in speciations	A10	0.025
$\kappa$	invasion pressure	Sec. A1.4	1.4